Effect of gravity on false-vacuum decay rates for O(4)-symmetric bubble nucleation

David A. Samuel and William A. Hiscock
Department of Physics, Montana State University, Bozeman, Montana 59717
(Received 22 May 1991)

The self-gravity of quantum fields is often considered to be a negligible perturbation upon a background spacetime and not of much physical interest. Its importance is determined by the ratio of the mass of the field to the Planck mass, this ratio being very small for those fields that we are most familiar in dealing with. However, it is conceivable that either in the very early Universe or even today a false-vacuum decay could occur associated with a field of appreciable mass. The effect of self-gravity upon false-vacuum decay was initially studied within the "thin-wall" approximation by Coleman and De Luccia. Their analysis involved the approximate solution of the coupled Euclideanized field and Einstein equations with the assumption of O(4)-symmetric bubble nucleation. In this paper we consider the range of validity of the "thin-wall" approximation by comparing the Coleman–De Luccia results with exact numerical results for a quartic polynomial potential. We also extend the analysis into regimes for which the "thin-wall" approximation is inapplicable. In the case of an initially de Sitter space decaying into Minkowski space, we find a smooth transition between the Coleman–De Luccia mode of bubble formation and the Hawking-Moss transition, wherein the entire spacetime tunnels "at once" to the maximum of the potential. In the case of the decay of an initially Minkowski space to an anti–de Sitter space, we find that there is a "forbidden region" of vacuum potential parameters for which decay is not possible. At energies far below the Planck scale, the boundary of this region is accurately described by the thin-wall prediction obtained by Coleman and De Luccia. At energies near the Planck scale, however, the actual "forbidden region" is significantly smaller than predicted by the thin-wall approximation; thus, vacuum decays are possible which appear to be forbidden by thin-wall calculations. In all cases, the inclusion of gravitational effects tends to thicken the wall of the bubble.

I. INTRODUCTION

Vacuum phase transitions play an important role in the theories of elementary-particle physics and cosmology. These include the "standard-model" quark-hadron phase transition and electroweak transition as well as more speculative transitions associated with grand unified theories (GUT's), supersymmetry and possible symmetry breaking in quantum gravity. One of the most important applications of such phase transitions is in the inflationary models of the early Universe. Such models are of interest as they possess an early de Sitter–like state in which the Universe undergoes exponential growth. Inflation could solve several of the contemporary puzzles of cosmology, e.g., the horizon, flatness, and monopole problems. However, it is obviously necessary for the Universe to evolve out of this de Sitter state as we find ourselves today living in a Universe with zero (or very small) vacuum energy density. In several models of inflation ("old" inflation, extended inflation), this evolution is believed to occur via a first-order phase transition in various of the quantum fields existing within the Universe. These fields provide a driving force for the early de Sitter state by having a nonzero vacuum energy density. However, during the phase transition the fields tunnel to a state having zero vacuum energy density and hence place the Universe into the Robertson-Walker state that we observe today.

False-vacuum decay associated with a first-order phase transition proceeds via nucleation of bubbles of true vacuum within the medium of false vacuum. These bubbles then expand, converting the Universe to a new phase. For first-order phase transitions in everyday matter, the nucleating bubbles are created as a result of statistical fluctuations within the medium. In zero-temperature quantum field theory, however, such bubbles are created as a result of quantum fluctuations. In the absence of gravity one may calculate the false-vacuum decay rate (i.e., the bubble nucleation rate per unit four volume) via the solution of the Euclideanized field equations with the appropriate boundary conditions. Such a solution gives the field configuration (in Euclidean space) of a nucleating bubble of a true vacuum. The false-vacuum decay rate per unit four-volume may then be expressed as $\Gamma = A\exp(-B)$, where B is the difference between the Euclidean action for the spacetime with the bubble and the spacetime without the bubble; the coefficient A typically has a magnitude given by the field mass to the fourth power. Coleman [1] has developed an approximation scheme for determining such decay rates in the situation where the difference between the energy density of the true- and false-vacuum states is small. When this is the case the nucleating bubbles are found to have a well-defined core of a true vacuum, a thin wall in which the field evolves rapidly from the true vacuum to false vacuum and an exterior of false vacuum (hence, the name "thin-wall" approximation).

As the vacuum phase transitions are taking place in a cosmological setting where gravity plays an inherently important role, we may ask whether the self-gravity of the quantum fields undergoing the phase transition will have an effect on the transition rate. This question has been addressed within the thin-wall approximation by Coleman and De Luccia [2]. Their analysis involved the approximate solution of the coupled Euclideanized field and Einstein equations, and they specifically considered O(4)-symmetric bubble nucleation for the decays from de Sitter to Minkowski space and Minkowski to anti–de Sitter space. They found that gravitational effects enhanced the decay rate for the transition from de Sitter to Minkowski space, but impeded the transition from Minkowski to anti–de Sitter space. In fact, for the decay from Minkowski to anti–de Sitter space, there was found to be a forbidden region in parameter space where no O(4)-symmetric decays could occur.

It may be argued that such gravitational effects are generally negligible, as the importance of the self-gravity of a quantum field is dictated by the ratio of the mass of the field to the Planck mass. For example, the electroweak mass scale of 10^2 GeV is well below the Planck mass scale of 10^{19} GeV and thus one would expect gravity to play an insignificant role in the electroweak phase transition. However, spontaneous symmetry breaking, vacuum phase transitions, and field masses near the Planck mass are common features of current proposals in grand unification, as well as in many quantum gravity proposals, with or without unification. It is then conceivable that either in the very early Universe or today a vacuum phase transition could occur associated with a field of appreciable mass. It is therefore worthwhile to obtain a better understanding of the effects of gravity upon such processes.

In this paper we shall consider the range of validity of the thin-wall approximation by comparing the results of Coleman and De Luccia with exact numerical results. The analysis will also be extended beyond those regimes for which the thin-wall approximation is applicable in order to gain a better understanding of the effects of gravity in such decays. Similar comparisons have previously been made for O(4) vacuum decay in the absence of gravity [3].

Our analysis shall be based upon bubble nucleation for scalar fields with the quartic polynomial potential $U(\phi)=U_c+m^2\phi^2-\eta\phi^3+\lambda\phi^4$, which we shall refer to from now on as a $\phi^{2\text{-}3\text{-}4}$ potential. The reason for choosing such a potential is that it is the simplest polynomial potential that contains two vacuum states where we may independently vary the energy-density difference between the two vacua and the field distance between the true- and false-vacuum states. It is also the most arbitrary renormalizable tree-level potential.

The $\phi^{2\text{-}3\text{-}4}$ potential is initially converted to a dimensionless form and then reexpressed in terms of parameters that are more physical; the coupled Euclideanized field and Einstein equations are also expressed in dimensionless form. The analysis is specialized to the decay from de Sitter to Minkowski space and Minkowski to anti–de Sitter space, in a similar manner to that of Coleman and De Luccia [2]. The "thin-wall" results are evaluated for the $\phi^{2\text{-}3\text{-}4}$ potential; this then allows for the subsequent comparison with the exact numerical results.

We find that for the decay from de Sitter to Minkowski space there is a continuous evolution from the Coleman–de Luccia tunneling mode to the Hawking-Moss [4] tunneling mode, as the mass of the field is increased. The Hawking-Moss tunneling mode corresponds to the entire universe tunneling, at an instant (i.e., along a spacelike surface), from the false-vacuum state to the top of the potential barrier separating the true and false vacua. During the subsequent evolution, the field evolves classically from the top of the potential barrier to the true-vacuum state.

For the decay from Minkowski to anti–de Sitter space, we find a forbidden region in the parameter space describing the potential, where no decays are possible, in a similar manner to Coleman and De Luccia. For small field masses the range of potential parameters corresponding to the forbidden region is predicted very well by the Coleman–De Luccia thin-wall approximation. However, as the field mass approaches the Planck mass, we find the forbidden region to be smaller than that predicted by the thin-wall approximation. Thus there are false-vacuum decays which are possible, although they appear to be prohibited according to the thin-wall approximation calculations.

II. FALSE-VACUUM DECAY WITH GRAVITY

It will be instructive to review the thin-wall approximation with the inclusion of gravity, as formulated by Coleman and De Luccia [2], for the potential under consideration. This will provide us with explicit results with which we may compare the exact numerical results and hence determine the range of validity of the thin-wall approximation.

Consider a self-interacting scalar field with a $\phi^{2\text{-}3\text{-}4}$ potential,

$$U=U_c+m^2\phi^2-\eta\phi^3+\lambda\phi^4 \ , \tag{1}$$

with $U_c, m^2, \eta, \lambda \geq 0$. U_c shall be the value of the false-vacuum energy density, the false-vacuum state being located at $\phi=0$ (with an appropriate choice of parameters). Changing to the dimensionless variables $\psi=\phi/m$, $\tilde{\eta}=\eta/m$, and $\tilde{U}=U/m^4$ gives

$$\tilde{U}=\tilde{U}_c+\psi^2-\tilde{\eta}\psi^3+\lambda\psi^4 \ . \tag{2}$$

We reexpress this potential in terms of the more physical parameters ψ_+, the value of the field at the true vacuum, and $\tilde{\varepsilon}$, the dimensionless energy-density difference between the true- and false-vacuum states. As we shall specifically consider only decay from de Sitter to Minkowski space or decay from Minkowski to anti–de Sitter space, then we have a constraint placed upon $\tilde{U}_c$, the dimensionless false-vacuum energy density. For the decay from de Sitter to Minkowski space, $\tilde{U}_c=\tilde{\varepsilon}$, and for the decay from Minkowski to anti–de Sitter space, $\tilde{U}_c=0$. The potential is then

$$\tilde{U}=[\tilde{\varepsilon}]+\psi^2-2(2\tilde{\varepsilon}+\psi_+^2)\frac{\psi^3}{\psi_+^3}+(3\tilde{\varepsilon}+\psi_+^2)\frac{\psi^4}{\psi_+^4} \ . \tag{3}$$

The first term, in square brackets, is included if we are considering the decay from de Sitter to Minkowski space, but excluded for decay from Minkowski to anti–de Sitter space. Finally, we change variables one more time by defining a scaled field $\sigma=\psi/\psi_+$, such that the false vacuum is located at $\sigma=0$ and the true vacuum is located at $\sigma=1$; we also introduce a parameter $\omega=\tilde{\varepsilon}/\psi_+^2$. The potential then takes the final form

$$\tilde{U}=[\tilde{\varepsilon}]+[\sigma^2-2(2\omega+1)\sigma^3+(3\omega+1)\sigma^4]\psi_+^2 \ . \quad (4)$$

Figure 1 shows this potential for the decay from de Sitter to Minkowski space (with $\omega=0.1$ and $\psi_+=1.0$). The equivalent potential for decay from Minkowski to anti–de Sitter would be shifted vertically downward by an amount $\tilde{\varepsilon}$.

We next require the coupled Euclideanized field and Einstein equations. The vacuum decay rate per unit four-volume is given by $\Gamma=A\exp(-B)$, where B is the difference between the Euclidean action for the spacetime with the bubble and the Euclidean action for the spacetime without the bubble. For the decay from Minkowski space to anti–de Sitter space, the initial spacetime without the bubble (i.e., Minkowski space) has a vanishing Euclidean action, and hence B is given simply by the Euclidean action for the bubble. However, for the decay from de Sitter space to Minkowski space, the initial empty spacetime (i.e., de Sitter space) does not have a vanishing Euclidean action, and so it is necessary to evaluate a subtraction term in order to obtain B. The solution to the Euclideanized equations, when rotated back into the Lorentzian sector, will also describe the late time evolution of the bubble.

In the absence of gravity it has been shown [5] that O(4)-symmetric bubbles will have the smallest action and hence be the dominant mode for decay. This result has not been successfully extended to the situation where gravity is present, but it is generally believed to still hold. Thus we shall consider O(4)-symmetric bubble nucleation

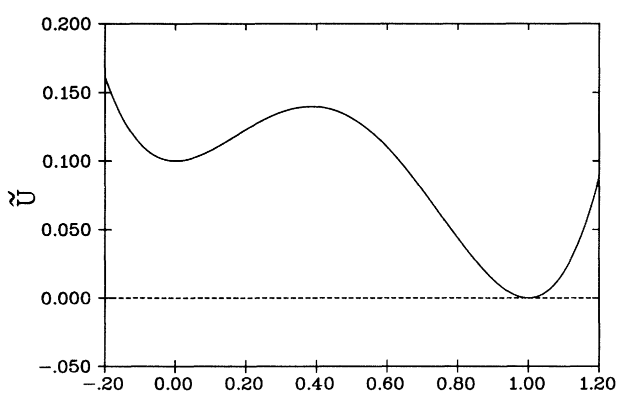

FIG. 1. Quartic polynomial potential, for the decay from de Sitter space to Minkowski space, with the scalar field defined such that the false vacuum occurs at $\sigma=0$ and the true vacuum at $\sigma=1$. The dimensionless energy-density difference $\tilde{\varepsilon}$ between the true- and false-vacuum states takes the value of 0.1 in this example.

in a similar manner to Coleman and De Luccia. The Euclideanized spacetimes that we are considering, i.e., de Sitter, Minkowski, and anti–de Sitter, are all O(4) symmetric, and so the appropriate line element for the Euclideanized spacetime is given by

$$ds^2=d\zeta^2+\nu(\zeta)^2d\Omega^2 \ , \quad (5)$$

where $d\Omega^2$ is the line element of the unit three-sphere. For (Euclideanized) de Sitter, Minkowski, and anti–de Sitter space, the function $\nu(\zeta)$ has the values $\kappa^{-1}\sin(\kappa\zeta)$, ζ, and $\kappa^{-1}\sinh(\kappa\zeta)$, respectively.

The Euclideanized scalar-field equation may be expressed as

$$g^{-1/2}\partial_\alpha(g^{1/2}g^{\alpha\beta}\partial_\beta)\phi=\frac{dU}{d\phi} \ , \quad (6)$$

where g is the determinant of the (Euclidean) metric. In terms of the coordinates of the line element given in Eq. (5) and knowing that for O(4) bubbles $\phi=\phi(\zeta)$, Eq. (6) reduces to

$$\frac{d^2\phi}{d\zeta^2}+\frac{3}{\nu}\frac{d\nu}{d\zeta}\frac{d\phi}{d\zeta}=\frac{dU}{d\phi} \ . \quad (7)$$

The stress-energy tensor for the scalar field acts as a source for the gravitational field. Assuming minimal coupling between the scalar and gravitational fields, the $G_{\zeta\zeta}$ component of Einstein's equation $G_{\alpha\beta}=8\pi GT_{\alpha\beta}$ is

$$\left[\frac{d\nu}{d\zeta}\right]^2=1+\frac{8\pi G}{3}\nu^2T_{\zeta\zeta} \ , \quad (8)$$

where

$$T_{\zeta\zeta}=\frac{1}{2}\left[\frac{d\phi}{d\zeta}\right]^2-U \ . \quad (9)$$

We again introduce dimensionless variables, $\xi=m\zeta$, $\rho=m\nu$, and make the additional substitution $G=1/m_P^2$, where m_P is the Planck mass. With these variables, using the expression in Eq. (4) for the potential, the Einstein equation may be written

$$(\rho')^2=1+\frac{8\pi}{3}\frac{m^2}{m_P^2}(\tfrac{1}{2}\sigma'^2-\{[\omega]+\sigma^2-2(2\omega+1)\sigma^3 +(3\omega+1)\sigma^4\})\rho^2\psi_+^2 \ , \quad (10)$$

where a prime indicates differentiation with respect to ξ. The Euclidean scalar-field equation then becomes

$$\sigma''+\frac{3\rho'}{\rho}\sigma'=2\sigma-6(2\omega+1)\sigma^2+4(3\omega+1)\sigma^3 \ . \quad (11)$$

The following boundary conditions are imposed upon Eqs. (10) and (11):

$$\rho=0 \quad \text{at } \xi=0 \quad (12)$$

for Eq. (10), and

$$\sigma'=0 \quad \text{at } \rho=0, \quad \sigma=0 \quad \text{at } \xi=\infty \quad (13)$$

for Eq. (11).

At this point we note a few invariances within the theory of O(4) vacuum decay with the $\phi^{2\text{-}3\text{-}4}$ potential. In the zero-gravity limit defined by $m_P \to \infty$, the solution to Eq. (10) reduces to $\rho = \xi$, and the solution to Eq. (11) depends only upon the single parameter ω. Thus the solution $\sigma(\xi)$ will be invariant under rescalings of $\tilde{\varepsilon}$ and ψ_+ provided the rescaling is performed in such a way as to keep $\omega = \tilde{\varepsilon}/\psi_+^2$ constant. This may be thought of as a consequence of only having one length scale in the theory (that given by the mass of the field).

When gravity is introduced (i.e., m_P is set to a finite value), the above symmetry is broken as we now have two natural length scales within the theory. However, there is still a similar but weaker symmetry within the theory. The coupled solutions $\sigma(\xi)$ and $\rho(\xi)$ remain invariant under the rescalings

$$m \to a^{1/2} m \ , \tag{14}$$

$$\tilde{\varepsilon} \to a^{-1} \tilde{\varepsilon} \ , \tag{15}$$

$$\psi_+ \to a^{-1/2} \psi_+ \ , \tag{16}$$

where a is an arbitrary constant. In the zero-gravity limit the m rescaling was unnecessary. The Euclidean action for the nucleating bubble will also be found to scale under these transformations:

$$S_E \to a^{-1} S_E \ . \tag{17}$$

The Euclidean action for the nucleating bubble has contributions from both the scalar-field potential and kinetic terms together with the gravitational Ricci scalar term:

$$S_E = \int d^4x \, g^{1/2} \left[\frac{1}{2} g^{\mu\nu} \partial_\mu \phi \partial_\nu \phi + U(\phi) + \frac{R}{16\pi G} \right] , \tag{18}$$

$$= 2\pi^2 \int d\xi \left\{ \nu^3 \left[\frac{1}{2} \left[\frac{d\phi}{d\xi} \right]^2 + U \right] + \frac{3}{8\pi G} \left[\nu^2 \frac{d^2\nu}{d\xi^2} + \nu \left[\frac{d\nu}{d\xi} \right]^2 - \nu \right] \right\} . \tag{19}$$

In determining the Euclidean action for the nucleating bubble, we may use the fact that the scalar field will be a solution to the coupled Euclideanized field and Einstein equations [Eqs. (10) and (11)]. Using the field equations to simplify Eq. (19), we find

$$S_E = -2\pi^2 \int d\xi \, \rho^3 \tilde{U} \ . \tag{20}$$

III. THIN-WALL ANALYSIS

The thin-wall approximation as presented by Coleman [1] makes use of the analogy between Eq. (11) and the classical motion of a particle of unit mass moving in the inverted potential $-\tilde{U}$, where σ corresponds to the particle's position and ξ to time. In the absence of gravity there is a "frictional" term in the equation of motion with the unusual frictional coefficient given by $(3/\xi)$, i.e., inversely proportional to the Euclidean time. When gravity is included this picture still holds but the frictional coefficient is more complicated, now being given by $(3\rho'/\rho)$.

The thin-wall approximation assumes that the field remains near to the top of the hill of the inverted potential (close to $\sigma = 1$) until ρ becomes very large, thus supposedly allowing the frictional coefficient to become arbitrarily small, as it is inversely proportional to ρ. Thus, when the field does eventually role off the hill, its subsequent motion is unaffected by friction. In this case the Euclideanized field equation may be written in an approximate form, by dropping the frictional term, thus making the equation more tractable.

When gravity is present the friction coefficient may be written as

$$\frac{3\rho'}{\rho} = 3 \left[\frac{1}{\rho^2} + \frac{8\pi}{3} \frac{m^2}{m_P^2} \left(\tfrac{1}{2}\sigma'^2 - \{ [\omega] + \sigma^2 - 2(2\omega+1)\sigma^3 + (3\omega+1)\sigma^4 \} \right) \psi_+^2 \right]^{1/2} . \tag{21}$$

Coleman and De Luccia claim that if ρ becomes large before the field rolls off the hill, the frictional coefficient [Eq. (21)] is very small and may be neglected. This is obviously true for the first term in Eq. (21), i.e., $1/\rho^2$. The second part of the frictional term does not depend upon ρ, however, its dependence being solely upon the shape of the potential and the mass of the scalar field. In the situation where the mass of the scalar field is very small, this second term will also be small and may be neglected in accordance with the analysis of Coleman and De Luccia. We shall see, however, that in the decay from Minkowski to anti–de Sitter space this second term plays a key role in determining the critical mass, after which there are no more allowed decays. This suggests that the analysis of Coleman and De Luccia may be inadequate for large mass fields in the region of criticality.

The thin-wall approximation in the presence of gravity requires some results from the approximation scheme in the absence of gravity. It shall be necessary to associate a degenerate potential $\tilde{U}_0(\sigma)$ with $\tilde{U}(\sigma)$ in such a way that $\tilde{U}_0(0) = \tilde{U}_0(1) = 0$ and $(d\tilde{U}_0/d\sigma)(0) = (d\tilde{U}_0/d\sigma)(1) = 0$. While in general there is no unique way to construct such a degenerate potential, if we accept the restriction of dealing with at most a quartic polynomial, then there is a unique degenerate potential, namely, that obtained from Eq. (4) by setting $\omega = 0$. We also subtract off the constant term in the potential $[\tilde{\varepsilon}]$ if it is present. Thus

$$\tilde{U}_0 = \sigma^2 (1 - \sigma^2) \psi_+^2 \ . \tag{22}$$

The thin-wall approximation requires us to evaluate the bubble wall action integral:

$$S_1 = \psi_+ \int_0^1 d\sigma (2\tilde{U}_0)^{1/2} \ . \tag{23}$$

The Euclidean action and radius of the nucleating bubble, for the thin-wall approximation scheme in the absence of gravity, are given by [1]

$$S_{\rm TW}=\frac{27\pi^2 S_1^4}{2\omega^3\psi_+^6} \tag{24}$$

and

$$\rho_0=\frac{3S_1}{\tilde{\varepsilon}} . \tag{25}$$

For the $\phi^{2\text{-}3\text{-}4}$ potential one finds

$$S_1=\psi_+^2\int_0^1[2\sigma^2(1-\sigma)^2]^{1/2}d\sigma=\frac{\psi_+^2}{3\sqrt{2}} , \tag{26}$$

while the Euclidean action becomes

$$S_{\rm TW}=\frac{\pi^2\psi_+^2}{24\omega^3} , \tag{27}$$

and the bubble radius is given by

$$\rho_0=\frac{1}{\sqrt{2}\omega} . \tag{28}$$

IV. DECAY FROM DE SITTER SPACE TO MINKOWSKI SPACE

In the presence of gravity the thin-wall results are modified because the approximate solution of the coupled Euclideanized field and Einstein equations are now required (for a complete derivation and explanation, see Coleman and De Luccia [2]). Their results are summarized here and evaluated for the $\phi^{2\text{-}3\text{-}4}$ potential. During the decay from de Sitter space to Minkowski space, the nucleating bubble radius is given by

$$\rho=\frac{\rho_0}{1+(\rho_0/2\Lambda)^2} , \tag{29}$$

where ρ_0 is the bubble radius in the absence of gravity [Eq. (25)] and Λ is the radius of curvature of the associated Euclideanized de Sitter space, which expressed in dimensionless form is given by

$$\Lambda^{-2}=\frac{8\pi m^2\tilde{\varepsilon}}{3m_P^2} . \tag{30}$$

The difference between the Euclidean action of the spacetime with and without the bubble (remembering that there will be a nonzero subtraction term associated with the empty de Sitter space) is

$$B=\frac{B_0}{[1+(\rho_0/2\Lambda)^2]^2} . \tag{31}$$

For the $\phi^{2\text{-}3\text{-}4}$ potential under consideration, the de Sitter to Minkowski space formulas (29) and (31) become

$$\rho=\frac{\psi_+^2}{\sqrt{2}\tilde{\varepsilon}}\left[1+\frac{\pi m^2\psi_+^4}{3m_P^2\tilde{\varepsilon}}\right]^{-1} \tag{32}$$

and

$$B=\frac{\pi^2\psi_+^8}{24\tilde{\varepsilon}^3}\left[1+\frac{\pi m^2\psi_+^4}{3m_P^2\tilde{\varepsilon}}\right]^{-2} . \tag{33}$$

Thus, as the mass of the field is increased, where $\tilde{\varepsilon}$ and ψ_+ are kept constant, the bubble radius decreases and the decay rate increases (i.e., there is a decrease in B). These results are now compared with the exact numerical results in order to estimate the validity of the approximation scheme.

There is an important difference between the false-vacuum decay from de Sitter to Minkowski space and false-vacuum decays both in the absence of gravity and in the decay from Minkowski to anti–de Sitter space. The spacetime outside a nucleating bubble is that of the false vacuum, and thus for the decay from de Sitter to Minkowski space the exterior spacetime is (Euclideanized) de Sitter space. This spacetime is closed and has the topology of a four-sphere. Thus there is a maximum value for ξ within this spacetime which occurs at the "south pole" of the four-sphere if the origin of coordinates $\xi=0$ is located at the "north pole." We may consider the nucleating bubble, without any loss of generality, to be centered on the north pole of this four-sphere. As a result, the boundary condition [Eq. (13)] requiring $\sigma\to 0$ as $\xi\to\infty$ is not valid for the decay of de Sitter space as this value of ξ is never attained in the Euclideanized de Sitter space; we therefore replace this boundary condition with the requirement that at the south pole (i.e., where ξ takes its maximum value) the field derivative σ' must vanish, for the same reason that this quantity must vanish at the north pole, namely, to prevent singular behavior in the Euclideanized field equation.

Figure 2 shows the evolution of the numerically integrated bubble profile as the mass of the field is increased, with the potential parameters $\tilde{\varepsilon}=0.5$ and $\psi_+=1.0$. We observe that, as the mass increases, the nucleating bubble profile flattens out and eventually reaches an equilibrium state where a further increase in the mass

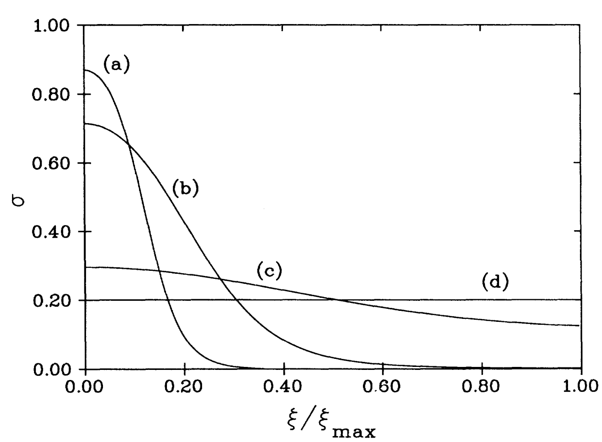

FIG. 2. Bubble profiles associated with the decay from de Sitter space to Minkowski space for several values of the field mass. The potential parameters $\tilde{\varepsilon}$ and ψ_+ are kept at the constant values of 0.5 and 1.0, respectively. The masses associated with the bubble profiles are (a) $m=0.1$, (b) $m=0.2$, (c) $m=0.3$, and (d) $m=0.4$. All bubble profiles with $m>0.4$ are well described by the Hawking-Moss mode; i.e., σ takes the constant value corresponding to the top of the inverted potential, $-\tilde{U}$.

has no effect upon the profile. The final state is described by the field having a constant value throughout the Euclideanized spacetime; this constant value corresponds to the field lying at the top of the potential barrier. This, however, is precisely the Hawking-Moss [4] tunneling mode. Thus, as the mass of the field is increased, the Coleman–De Luccia tunneling mode evolves continuously into the Hawking-Moss tunneling mode.

The Hawking-Moss tunneling mode corresponds to the entire universe tunneling "at once" from the false-vacuum state to the top of the potential barrier. This simply results in another de Sitter universe, though one that is unstable to field perturbations, with a larger vacuum energy density. After such a transition has taken place, quantum or other fluctuations push the field off the top of the potential hill and the field then evolves classically to the true-vacuum state. The expression for B corresponding to the Hawking-Moss mode is fairly easy to calculate, being just the volume of the respective Euclideanized de Sitter space multiplied by the associated energy density, and is given by

$$B_{\mathrm{HM}} = \frac{3m_P^4}{8m^4}(\tilde{\varepsilon}^{\,-1} - \tilde{\varepsilon}_{\mathrm{top}}^{\,-1}) \ . \tag{34}$$

The smooth evolution of the bubble profile from an approximately thin-wall bubble to the spatially homogeneous Hawking-Moss mode is certainly not evident from the thin-wall study of Coleman and De Luccia; the existence of such a transition, however, has been previously studied by Jensen and Steinhardt [6,7]. It might be argued that with $\tilde{\varepsilon}=0.5$ the thin-wall approximation is not valid anyway; however, a similar transition takes place

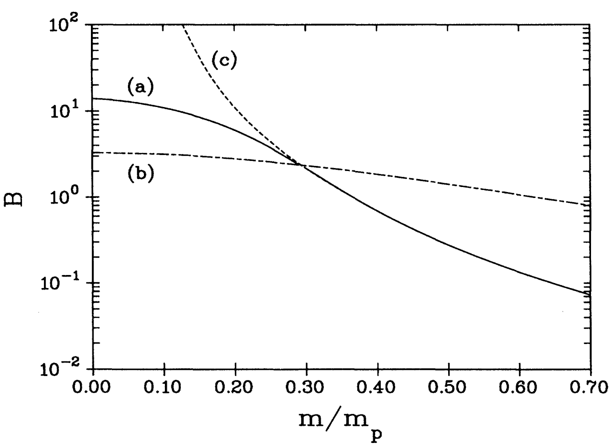

FIG. 3. Difference between the Euclidean action for the bubble spacetime and the empty spacetime (B) for the decay from de Sitter space to Minkowski space as a function of the field mass m, where the potential parameters $\tilde{\varepsilon}$ and ψ_+ are kept at the constant values of 0.5 and 1.0, respectively. Curve (a) shows the exact value of B obtained numerically, curve (b) shows B_{TW} corresponding to the thin-wall approximation, and curve (c) shows B_{HM} corresponding to the Hawking-Moss tunneling mode. $B_{\mathrm{exact}} \approx B_{\mathrm{HM}}$ for field masses above the "crossover" point, this being the point where $B_{\mathrm{TW}} = B_{\mathrm{HM}}$.

with values of $\tilde{\varepsilon}$ and m for which the thin-wall approximation is valid.

Though the transition from the Coleman–De Luccia mode to the Hawking-Moss mode is continuous, there do appear to be three distinct regimes associated with this decay.

As the mass is initially increased from zero, the end point for the bubble profile, i.e., $\sigma(\xi_{\max})$, remains very close to $\sigma=0$; we may characterize these as "strong" Coleman–De Luccia modes. Then, as the field mass continues to increase, a rapid transition occurs in which the end point of the bubble profile evolves rapidly from $\sigma=0$ to $\sigma=\sigma_{\mathrm{top}}$, where σ_{top} is the field value corresponding to the top of the potential barrier. Finally, we arrive at the Hawking-Moss mode where the bubble profile takes the constant value of σ_{top} throughout the spacetime. A further increase in the field mass does not change the characteristics of the nucleating bubble profile; i.e., the nucleating bubble always appears via the Hawking-Moss mode for larger field masses.

Figure 3 shows the difference between the Euclidean action for the bubble spacetime and the empty spacetime (i.e., B): (a) for the exact numerical bubble solutions, (b) for the thin-wall approximation, and (c) for the Hawking-Moss mode. The Hawking-Moss mode, for small field masses, has a larger action than that of the thin-wall approximation; however, as the field mass is increased, there is a crossover point, beyond which the Hawking-Moss action is smaller than the approximate action calculated from the thin-wall formalism.

The behavior of the exact action, determined numerically, is quite striking. For small field masses the exact action is qualitatively similar to the curve derived from the thin-wall approximation, with a finite value at $m=0$ and a gradual decrease as the mass of the field is increased (the two curves could be made *quantitatively* more similar by choosing a smaller value of $\tilde{\varepsilon}$). At the point defined by $B_{\mathrm{HM}} = B_{\mathrm{TW}}$, the phase transition process undergoes what may be described as a "crossover" in the mode by which the phase transition proceeds; beyond this point, $B_{\mathrm{exact}} \approx B_{\mathrm{HM}}$. This behavior is quite remarkable as the thin-wall approximation does not (and cannot) even hint at this transition; thus the "crossover mass" at which $B_{\mathrm{HM}} = B_{\mathrm{TW}}$ provides an upper limit on the scalar-field mass for which the thin-wall approximation has any validity.

It is worth noting the relationship between the transition in B and the corresponding bubble profile evolution. For this example a field mass $m=0.3$ places B_{exact} in the Hawking-Moss region; however, the bubble profile for $m=0.3$ [Fig. 2, curve (c)] has not yet fully transformed to the Hawking-Moss form. This may be explained by the fact that the Hawking-Moss solution corresponds to the field lying at an extremum of the potential; thus, first-order variations of the field about this extremum result in higher-order variations in B (remembering that B involves the integral of the field potential for the nucleating bubble throughout the spacetime). Hence the bubble profile for $m=0.3$ gives a value for B extremely close to the Hawking-Moss value because its profile is only a small variation away from the Hawking-Moss solution.

V. DECAY FROM MINKOWSKI SPACE TO ANTI–DE SITTER SPACE

Associated with the decay from Minkowski space to anti–de Sitter space, the thin-wall formulas for the bubble radius and Euclidean action are

$$\rho = \frac{\rho_0}{1-(\rho_0/2\Lambda)^2} \tag{35}$$

and

$$B = \frac{B_0}{[1-(\rho_0/2\Lambda)^2]^2} . \tag{36}$$

With an initially empty Minkowski spacetime, the difference between the Euclidean action for the spacetime with and without the bubble reduces to simply the Euclidean action for the bubble spacetime; i.e., there is no nonzero subtraction term.

For the $\phi^{2\text{-}3\text{-}4}$ potential, Eqs. (35) and (36) become

$$\rho = \frac{\psi_+^2}{\sqrt{2}\tilde{\varepsilon}} \left[1 - \frac{\pi m^2 \psi_+^4}{3 m_P^2 \tilde{\varepsilon}} \right]^{-1} \tag{37}$$

and

$$B = \frac{\pi^2 \psi_+^8}{24 \tilde{\varepsilon}^3} \left[1 - \frac{\pi m^2 \psi_+^4}{3 m_P^2 \tilde{\varepsilon}} \right]^{-2} . \tag{38}$$

Equation (38) implies that for the decay from Minkowski to anti–de Sitter space the bubble radius and action may become infinite for some potentials. In particular, if we keep $\tilde{\varepsilon}$ and ψ_+ constant and increase the mass of the scalar field from zero, then a critical mass will be reached, at which point the action becomes infinite and the decay rate goes to zero; no bubble solutions will exist for greater field masses. Alternatively, if we keep both the mass of the field and the dimensionless field distance between the two vacuum states constant, then a reduction in $\tilde{\varepsilon}$ will also bring about this singular behavior in B and prevent any subsequent vacuum decay.

The critical mass in this situation is given by

$$m_c = \frac{1}{\psi_+^2} \left[\frac{3\tilde{\varepsilon}}{\pi} \right]^{1/2} m_P . \tag{39}$$

For most fields that we are familiar with, the dimensionless quantities $\tilde{\varepsilon}$ and ψ_+ will typically be of order unity, or, at most, a few orders of magnitude. Thus, from Eq. (39), we see that the associated critical mass will be close to the Planck mass and certainly well away from the masses that we observe for fields today.

Coleman and De Luccia (see also Weinberg [8]) explain this divergence of the Euclidean action in terms of the requirement that the nucleating bubble solution have zero energy. For the decay from Minkowski to anti–de Sitter space, the gravitational corrections to the energy result in the bubble having a larger radius than in the zero-gravity limit, because the net gravitational contribution to the energy is positive. At the critical mass the gravitational corrections result in the bubble having an infinite radius, and above that mass there is no radius at which the negative volume energy density of the true vacuum can overcome the positive gravitational corrections to result in a bubble of zero total energy.

We shall now consider the exact numerical results to see how they compare to the thin-wall approximation.

Figures 4 and 5 show the evolution of a nucleating bubble profile as the mass of the field is increased, with the potential parameters being fixed at $\tilde{\varepsilon}=0.5$ and $\psi_+=1.0$; these obviously do not correspond to thin-wall profiles. We note that as the mass of the field approaches the critical value the starting point for the field [i.e.,

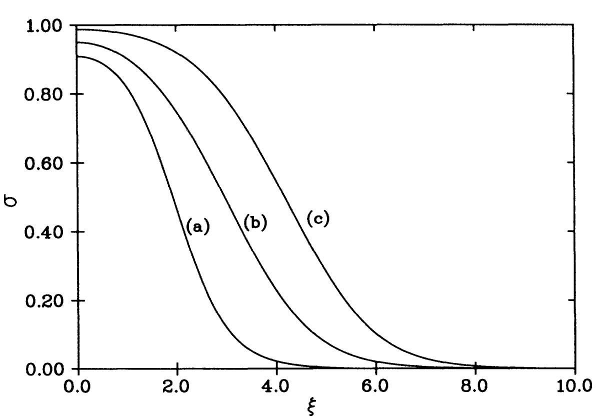

FIG. 4. Bubble profiles $\sigma(\xi)$ for the decay from Minkowski space to anti–de Sitter space for several values of the field mass. The potential parameters $\tilde{\varepsilon}$ and ψ_+ are kept at the constant values of 0.5 and 1.0, respectively. The masses of the field for the three curves are (a) $m=0$, (b) $m=0.82$, and (c) $m=0.85$. The critical mass m_c is approximately 0.865 for this choice of potential parameters, and so curves (b) and (c) show the changes in the bubble profile as criticality is approached.

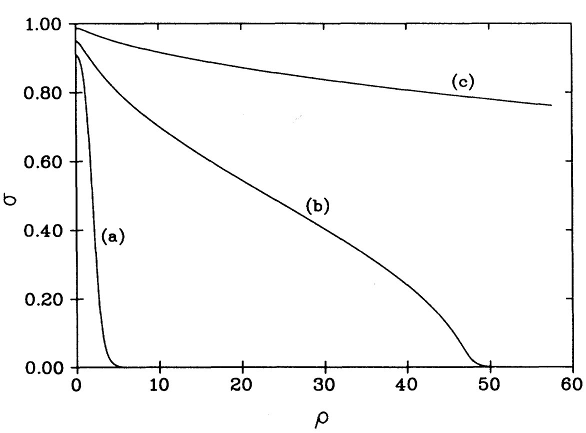

FIG. 5. Bubble profiles $\sigma(\rho)$ for the decay from Minkowski space to anti–de Sitter space. The potential and mass parameters for the three curves are the same as for Fig. 4. The $\sigma(\rho)$ profile evolution has a marked difference to the $\sigma(\xi)$ profile evolution as criticality is approached, which may be explained in terms of the solution curves of the Einstein equations, shown in Fig. 6.

$\sigma(\rho=0)]$ approaches a limiting value of 1.0. This may be explained quite easily within the "rolling off the hill of the inverted potential" analogy: As the mass of the field is increased, then from Eq. (21) we see that the magnitude of the frictional term is increased. Thus more energy is required to reach the final point of $\sigma(\rho\rightarrow\infty)=0$, and so the field has to start from a higher point on the hill. If the mass of the field becomes sufficiently large, then we could expect the frictional term to be sufficient to prevent the field from ever reaching $\sigma=0$ at any finite value of ρ.

In the absence of gravity the frictional term was inversely proportional to the Euclidean time, and so there was always a value of ρ for which the frictional term was small enough so that the field could "roll off the hill" and reach $\sigma=0$. However, in the presence of gravity the frictional term contains a piece which does not depend upon ρ and is only a function of the field mass and shape of the potential. Therefore, the thin-wall approximation strategy of waiting long enough in Euclidean time for the friction to become negligible will not always work with gravity present.

The bubble profiles $\sigma(\rho)$ undergo a dramatic evolution as the mass of the field is increased; this may be explained with reference to the solution curves $\rho(\xi)$ for the Einstein equation, shown in Fig. 6. For all decays from Minkowski space to anti–de Sitter space, there will be a potential barrier which has a corresponding positive energy density. Thus, when the bubble profile evolves through this barrier, the spacetime will undergo a de Sitter–like stage of evolution. This appears in the $\rho(\xi)$ profiles as a flattening out of the curves, and this phenomenon increases in prominence as the mass of the field is increased. Eventually, if the mass of the field is increased sufficiently, there will be a point in the $\rho(\xi)$ profile where $\rho'=0$. This may be thought of as the bubble profile running into a de Sitter horizon (of course, in the Euclidean signature space this is more accurately described as an "equator"). The initial appearance of such a point in the bubble profile defines the critical mass associated with the decay from Minkowski to anti–de Sitter space.

Figure 7 shows the critical mass as a function of $\tilde{\varepsilon}$, the lower curve corresponding to the thin-wall approximation critical line and the upper curve corresponding to the exact critical line. For small $\tilde{\varepsilon}$, which is the domain in which one would expect the thin-wall approximation to be accurate, the thin-wall approximation gives a remarkably good prediction for the critical mass as is illustrated by the exact critical line being asymptotic to the approximate critical line in this region. Beyond the domain of validity of the thin-wall approximation, the exact critical line diverges from the approximate critical line, such that the exact critical mass always lies above the approximate critical mass. Thus there are vacuum decays which the thin-wall approximation would label as forbidden, but which could actually occur.

Figure 8 shows the evolution of the ratio of $B_{\rm TW}$ to $B_{\rm exact}$ as the mass for the field is increased, where the potential parameter ψ_+ is kept at 1.0 and $\tilde{\varepsilon}$ takes on the values 0.1, 0.3, and 0.5 for the three curves (a), (b), and (c), respectively. We observe that the thin-wall approximation initially underestimates B (and hence overestimates the vacuum decay rate), though the agreement with $B_{\rm exact}$ improves as $\tilde{\varepsilon}$ is decreased, as expected. As the mass of the field is increased $B_{\rm TW}$ is found to diverge before $B_{\rm exact}$; this occurs because the critical mass for the thin-wall approximation always lies below the exact critical mass.

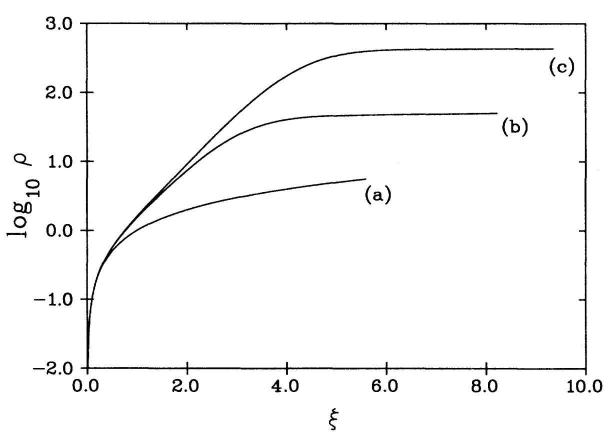

FIG. 6. Solution curves for the Einstein equation giving the $\rho(\xi)$ evolution for the three bubble profiles shown in Figs. 4 and 5. As criticality is approached, the ρ evolution reaches a "plateau" which may be pictured as the bubble profile "running into a de Sitter horizon" (a point where $\rho'=0$). The plateau corresponds to a de Sitter phase of evolution and occurs when the bubble profile runs through the potential barrier where the energy density is positive.

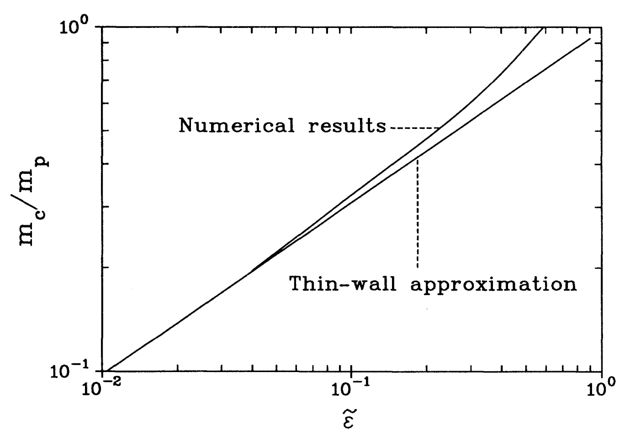

FIG. 7. Critical mass associated with the decay from Minkowski space to anti–de Sitter space, above which no O(4)-symmetric decays are permitted. The lower curve shows the critical mass line derived from the thin-wall approximation and the upper curve shows the exact critical mass line obtained numerically. In the thin-wall regime, corresponding to a small value of $\tilde{\varepsilon}$, the exact critical mass asymptotically approaches the value given by the thin-wall approximation and there is good agreement between the exact results and approximate results. Away from the thin-wall regime, as $\tilde{\varepsilon}$ becomes larger, the exact critical line deviates and lies above the approximate critical line.

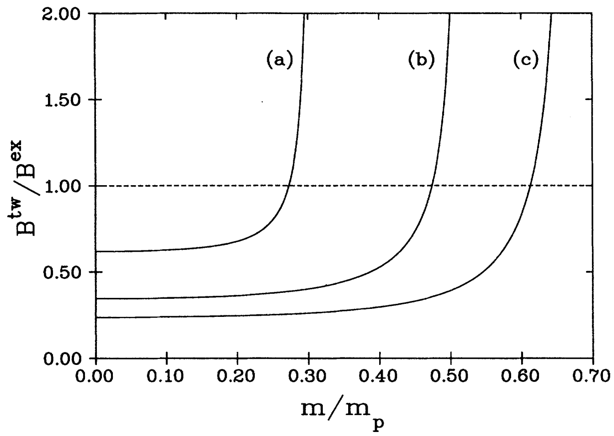

FIG. 8. Evolution of the ratio of $B_{\rm TW}$ to $B_{\rm exact}$, for the decay from Minkowski space to anti–de Sitter space, as the mass of the field is increased. The three curves have different values of $\bar{\epsilon}$ given by (a) $\bar{\epsilon}=0.1$, (b) $\bar{\epsilon}=0.3$, and (c) $\bar{\epsilon}=0.5$; $\psi_+=1.0$ in all three cases. The thin-wall approximation initially underestimates B. As the thin-wall critical mass lies below the exact critical mass, the thin-wall expression for B diverges prior to the divergence in the exact value for B.

Figure 9 shows the evolution of the ratio of the thin-wall bubble radius to the exact bubble radius for the same set of parameters as in Fig. 8. We define the bubble radius to be $\rho(\sigma_{\rm initial}/2)$, where $\sigma_{\rm initial}$ is the starting value of σ at $\rho=0$. The qualitative behavior of the bubble radius evolution is very similar to that of the evolution of B, the divergence in the thin-wall radius again occurring before the exact divergence as a result of the thin-wall critical mass lying below the exact critical mass.

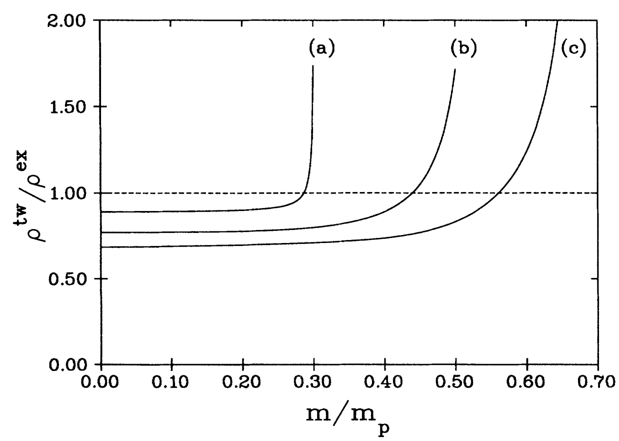

FIG. 9. Evolution of ratio of the bubble "radius" computed in the thin-wall approximation to the exact bubble radius [defined as $\rho(\sigma_{\rm initial}/2)$, where $\sigma_{\rm initial}$ is the starting value of σ at $\rho=0$] for the decay from Minkowski space to anti–de Sitter space, as the mass of the field is increased. The three curves have different values of $\bar{\epsilon}$ given by (a) $\bar{\epsilon}=0.1$, (b) $\bar{\epsilon}=0.3$, and (c) $\bar{\epsilon}=0.5$; $\psi_+=1.0$ in all three cases. The qualitative behavior here is similar to that of the evolution of B, shown in Fig. 8.

VI. CONCLUSION

The exact numerical solutions to the coupled Euclideanized field and Einstein equations certainly throw more light onto the effect of self-gravity upon false-vacuum decay than is provided solely from the results of the thin-wall approximation. There are also predictions of the qualitative behavior that are quite different from the thin-wall behavior, though these may be argued to lie beyond the region of applicability of the approximation scheme.

For the decay from de Sitter space to Minkowski space, we observe a transition from the Coleman–De Luccia thin-wall tunneling mode to the Hawking-Moss tunneling mode as the mass of the field is increased. This transition, though a continuous evolution, predominantly occurs in the parameter range where the Euclidean actions for the Hawking-Moss and Coleman–De Luccia thin-wall approximation tunneling modes are equal. For a given field mass, the exact tunneling mode appears to favor the "mechanism" which corresponds to the approximate tunneling mode with the smallest Euclidean action. Thus, for small field masses, where the Coleman–De Luccia thin-wall mode has a smaller Euclidean action than the Hawking-Moss mode, the exact tunneling mode has the characteristics of the Coleman–De Luccia mode. For large field masses, where the Hawking-Moss tunneling mode has the smaller Euclidean action, the exact tunneling mode has the Hawking-Moss characteristics. It should be remembered that both the Coleman–De Luccia and Hawking-Moss "modes" and actions are approximations to the exact solutions we have obtained numerically.

For the decay from Minkowski space to anti–de Sitter space, the thin-wall approximation prediction of the existence of a region of "forbidden decays" in the potential parameter space was found to be correct. For a fixed shape of potential, there is a maximum mass scale for the potential, beyond which no further decays occur. The thin-wall critical mass curve is found to be a very good approximation to the actual boundary of this forbidden decay region, even beyond the domain in which the thin-wall approximation is applicable. When the thin-wall approximation to the boundary deviates from the exact boundary of the forbidden decay region, it is always such that the approximate critical mass lies below the exact critical mass. As a result, some decays which appear to be forbidden according to the thin-wall approximation may actually proceed.

For both the decays from de Sitter to Minkowski space and from Minkowski to anti–de Sitter space, gravity is seen to have the effect of "thickening" the bubble walls, thus transforming bubbles which in the absence of gravity would be regarded as thin-walled to thick-walled bubbles in the presence of gravity.

ACKNOWLEDGMENTS

This research was supported in part by National Science Foundation Grant Nos. PHY88-03234 and RII-8921978.

[1] S. Coleman, Phys. Rev. D **15**, 2929 (1977).
[2] S. Coleman and F. De Luccia, Phys. Rev. D **21**, 3305 (1980).
[3] D. A. Samuel and W. A. Hiscock, Phys. Lett. B **261**, 251 (1991).
[4] S. W. Hawking and I. G. Moss, Phys. Lett. **110B**, 35 (1982).
[5] S. Coleman, V. Glaser, and A. Martin, Commun. Math. Phys. **58**, 211 (1978).
[6] L. G. Jensen and P. J. Steinhardt, Nucl. Phys. **B237**, 176 (1984).
[7] L. G. Jensen and P. J. Steinhardt, Nucl. Phys. **B317**, 693 (1989).
[8] S. Weinberg, Phys. Rev. Lett. **48**, 1776 (1982).